Modeling boreal forest evapotranspiration and water balance at stand and catchment scales: a spatial approach.

Samuli Launiainen[1], Mingfu Guan[2,1], Aura Salmivaara[1], and Antti-Jussi Kieloaho[1]

[1]Nature Resources Institute Finland, Latokartanonkaari 9, 00790 Helsinki, Finland
[2]Department of Civil Engineering, The University of Hong Kong, HKSAR, China

Correspondence: Samuli Launiainen (samuli.launiainen@luke.fi)

Supplementary material

1 Supplementary figures and tables

Supplementary material is provided below to support interpretation of the manuscript.

For details how to set up and run the model, please see the model code and brief user manual at https://github.com/lukeecomod/spafhy_v1.

The figures and tables are referred as Fig. or Table Sx in the main paper

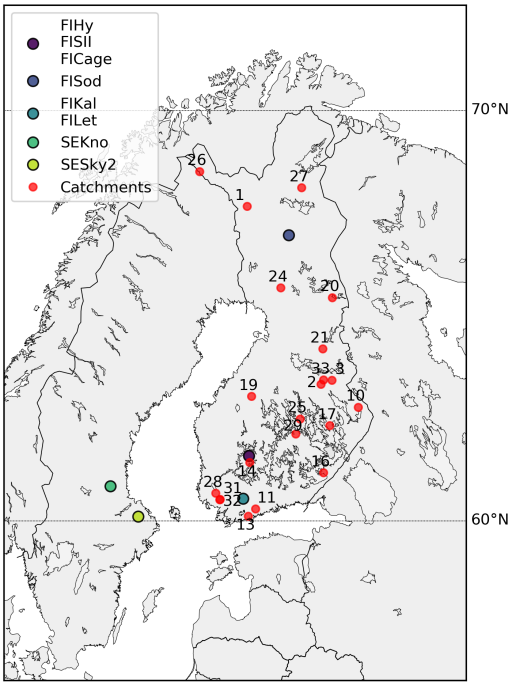

Figure 1. Location of the eddy-covariance sites (Table 1) and the 21 headwater catchments (Table S1) used in this study.

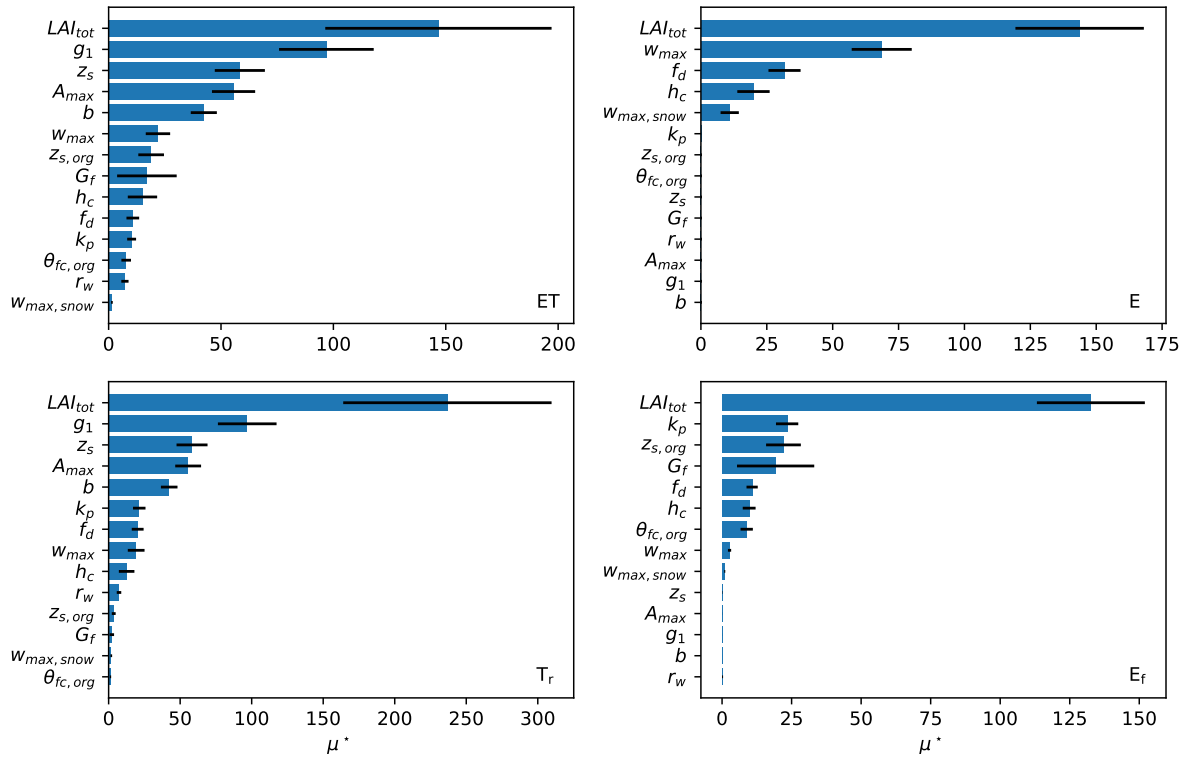

Figure 2. Parameter ranking based on mean of absolute values ($\mu_\star$) of the distribution of elementary effects for evapotranspiration (ET), transpiration (T_r), evaporation from canopy interception (E), and ground evaporation (E_f). The higher the $\mu_\star$ the more influential the parameter is. Error bars are 95% confidence intervals based on re-sampling (N=1000).

Table 1. Soil types and their hydraulic properties used in the simulations. The θ_s is porosity, θ_{fc} and θ_{wp} volumetric water contents at field capacity and wilting point, K_{sat} saturated hydraulic conductivity and β parameter describing power-law decay of hydraulic conductivity with decreasing saturation ratio.

Type	θ_s (m^3m^{-3})	θ_{fc} (m^3m^{-3})	θ_{wp} (m^3m^{-3})	K_{sat} (m s^{-1})	β (-)
Coarse textured	0.41	0.21	0.10	1.0×10^{-4}	3.1
Medium textured	0.43	0.33	0.13	1.0×10^{-5}	4.7
Fine textured	0.50	0.34	0.25	1.0×10^{-6}	7.9
Peat	0.90	0.41	0.11	5.0×10^{-5}	6.0

Coarse textured includes sand, sandy till and gravelly till soils. Medium textured cover soil types from fine finesand and silty tills to finesandy till. Fine textured represents clays and silt. Hydrological properties correspond to sand, and silty loam and clay in Bittelli et al. (2015), respectively.

Table 2. Characteristics of headwater-catchments used in model validation

Ch.	Name	Lat, Lon	Area (ha)	$\langle LAI \rangle$ (m^2m^{-2})	σ_{LAI} (m^2m^{-2})	f_d	Vol. (m^3ha^{-1})	$\langle TWI \rangle$	β_{TWI}	fine text. (-)	medium (-)	coarse (-)	peat (-)	m (m)	d_j (-)	Years
C1	Lompolojänganoja	68.00N, 24.20E	513.4	2.3	1.07	0.26	63.86	8.31	0.18	0	0.71	0.04	0.25	0.025	0.69	2014, 2015
C2	Liuhapuro	63.76N, 28.51E	166.48	4.4	1.92	0.21	157.42	8.04	0.2	0	0.35	0	0.65	0.006	0.74	2006, 2008
C3	Porkkavaara	63.86N, 29.16E	71.58	4.3	1.64	0.19	167.58	7.02	0.23	0	0.79	0.01	0.2	0.026	0.72	2006-2015
C10	Kelopuro	63.16N, 30.69E	71.6	1.8	1.36	0.11	86.94	8.35	0.27	0	0.39	0	0.61	0.011	0.68	2006-2013
C11	Metsäpuro	60.35N, 24.69E	128.5	4.6	1.61	0.27	182.18	6.46	0.28	0.12	0.83	0	0.05	0.012	0.74	2015
C13	Rudbäcken	60.14N, 24.26E	433.1	3.5	2.22	0.3	139.75	6.91	0.26	0.22	0.7	0.02	0.06	0.007	0.68	2015
C14	Paunulanpuro	61.66N, 24.34E	154.0	4.4	1.75	0.3	166.61	7.42	0.24	0.07	0.8	0	0.13	0.007	0.68	2007-2015
C16	Huhtisuonoja	61.38N, 28.65E	505.4	3.3	1.39	0.24	152.25	8.24	0.27	0	0.25	0.26	0.49	0.007	0.68	2007-2015
C17	Kesselinpuro	62.67N, 29.03E	2005.7	3.7	2.04	0.32	140.18	8.09	0.26	0.01	0.61	0	0.38	0.006	0.70	2006-2015
C19	Pahkaoja	63.45N, 24.45E	2321.8	1.7	1.35	0.25	65.34	8.81	0.24	0	0.44	0.04	0.52	0.006	0.72	2008-2011, 2013-2015
C20	Vääräjoki	65.91N, 29.18E	1831.2	1.9	1.61	0.24	54.3	7.87	0.26	0	0.51	0.01	0.48	0.009	0.64	2006-2015
C21	Myllypuro	64.66N, 28.62E	1047.0	3.1	1.54	0.29	96.45	7.54	0.22	0	0.66	0	0.34	0.01	0.63	2006-2010, 2012-2015
C24	Kotioja	66.14N, 26.15E	1715.8	1.9	1.5	0.25	50.87	8.67	0.22	0	0.45	0.01	0.54	0.007	0.76	2006-2015
C25	Kohisevanpuro	62.85N, 27.28E	1070.0	3.6	2.18	0.33	135.71	7.66	0.25	0	0.7	0	0.3	0.01	0.69	2006-2015
C26	Iittovuoma	68.74N, 21.41E	1157.1	0.2	0.4	0.91	2.41	7.42	0.22	0	0.86	0.01	0.12	0.02	0.76	2006-2015
C27	Laanioja	68.40N, 27.39E	1370.6	0.7	0.64	0.37	24.2	7.65	0.21	0	0.87	0.06	0.06	0.014	0.76	2006-2015
C28	Kroopinsuo	60.80N, 22.37E	179.1	3.3	1.38	0.18	144.37	7.28	0.26	0	0.71	0	0.29	0.006	0.62	2014-2015
C29	Surnui	62.45N, 27.03E	70.8	2.8	1.72	0.34	107.52	7.92	0.22	0	0.59	0.04	0.37	0.009	0.62	2015
C31	Ojakorpi	60.63N, 22.62E	31.1	3.5	1.57	0.27	140.48	7.18	0.25	0	0.95	0	0.05	0.006	0.65	2012-2015
C32	Rantainrahka	60.61N, 22.60E	36.4	3.4	1.71	0.18	143.76	7.44	0.23	0.03	0.88	0	0.08	0.008	0.61	2013-2015
C33	Kivipuro	63.87N, 28.65E	50.5	4.0	1.29	0.27	132.6	7.96	0.2	0	0.54	0	0.46	0.009	0.66	2006-2009, 2012, 2014-2015

C is the catchment number (Fig. S1); $\langle LAI \rangle$ and σ_{LAI} are mean and standard deviation of 1-sided leaf-area index; f_d the mean contribution of deciduous trees to LAI; Vol. the mean tree volume; $\langle TWI \rangle$ and β_{TWI} characterize the mean and standard deviation of log-normal distribution fitted to the discrete topographic wetness index (TWI) distribution.

Fine, medium, coarse and peat: proportion (-) of grid cells belonging to soil type classes in Table 2 of the main document; m - Topmodel parameter effective soil depth; d_j objective function value (eq. 22).

2 Aerodynamic and surface conductances

The attenuation of mean wind speed U within the canopy is assumed exponential

$$U(z) = U(h_c)\, exp^{\alpha\,(z/h_c - 1)}, \tag{1}$$

where α (-) is attenuation coefficient, h_c (m) canopy height and z height above the ground. Neglecting effects of diabatic stability, the wind speed at canopy top $U(h_c)$ can be estimated from wind speed U_m at reference height z_m (typically 2 or 10 m) using logarithmic wind profile yielding

$$U(h_c) = U_m \frac{ln[(z_m - d)/z_{om}]}{ln[(h_c - d)/z_{om}]}, \tag{2}$$

where $d \sim 0.66\, h_c$ is displacement height and $z_{om} \sim 0.123 h_c$ the roughness height for momentum.

The resistance for turbulent transport in the canopy air space r_a (Magnani et al., 1998)

$$r_a = \frac{1}{k_v^2 U_o} ln[(z_m - d)/z_{om}]\, ln[(z_m - d)/z_{ov}, \tag{3}$$

where $k_v \sim 0.41$ is the von Karman constant and $z_{ov} \sim 0.1\, z_{om}$ the roughness height for water vapor.

Representation for canopy-level quasi-laminar boundary-layer resistance r_b, assuming uniform leaf-area distribution and exponential wind profile within canopy, has been derived by Choudhury and Monteith (1988)

$$r_b = \frac{1}{LAI}\, \beta \sqrt{\frac{w}{U(h_c)} \frac{\alpha}{[1 - exp^{-0.5\alpha}]}}, \tag{4}$$

where w is characteristic leaf width (here 0.01 m) and proportionality coefficient $\beta \sim 285$ s m^{-1} (Campbell and Norman, 1998). The canopy aerodynamic conductance is computed assuming r_a and r_n act on series

$$G_{a,c} = \frac{1}{r_a + r_b}. \tag{5}$$

The surface conductance for sublimation of intercepted snow, G_i,follows Essery et al. (2003) and Best et al. (2011)

$$G_i = \frac{3 C_e\, D_w\, Sh W}{2 \rho_i\, r^2} \sim \frac{C_e\, Sh W}{7.68}, \tag{6}$$

where $Sh = 1.79 + 3U^{0.5}$ is the Sherwood number, ρ_i density of ice, D_w molecular diffusivity of water vapor in the air, and r the characteristic radius of snow grains (500 μm). The exposure coefficient C_e

$$C_e = k_1 \left(\frac{W}{W_{max}} \right)^{-0.4} \tag{7}$$

depends on amount of intercepted snow water W relative to the maximum storage and $k_1 = 0.01$ from Pomeroy et al. (1998).

The forest floor / peatland surface resistance is computed as

$$r_{a,f} = \frac{1}{k_v^2 U_g} ln(z_g/z_{os})\, ln(z_g/z_{osv}), \tag{8}$$

where U_g is the wind speed at height z_g above ground (from eq. 1), and z_{os} and z_{osv} surface roughness heights for momentum and water vapor, respectively. Finally, the forest floor conductance $G_{a,f} = 1/r_{a,f}$.

3 Deriving parameter ranges for eq. 4: test against a common gas-exchange model

In the main paper, eq. 4 provides approach to estimate the canopy conductance G_c based on well-established stomatal conductance model, simplified canopy radiation transfer scheme and stand LAI. The stomatal model used is based on Medlyn et al. (2012), who showed that leaf-scale stomatal conductance (g_s, mol m-2 s-1) is related to leaf net photosynthetic rate (A, μmol $\mathrm{m^{-2}s^{-1}}$) as

$$g_s \simeq g_o + 1.6\left(1+\frac{g_1}{\sqrt{D}}\right)\frac{A}{C_a}, \tag{9}$$

where C_a is the atmospheric CO_2 mixing ratio (ppm), D (kPa) is vapor pressure deficit, g_o residual (or cuticular) conductance and g_1 a species-specific parameter that depends on plant water use strategy. Noting that $g_o \ll g_s$ (Medlyn et al., 2012) and representing photosynthetic light response by saturating hyperbola (Saugier and Katerji, 1991), eq. (9) can be approximated as

$$g_s = 1.6\left(1+\frac{g_1}{\sqrt{D}}\right)\frac{A_{max}}{C_a}\frac{PAR}{PAR+b}C_{air}, \tag{10}$$

where A_{max} (μ mol $\mathrm{m^{-2}\ s^{-1}}$) is the light-saturated photosynthesis rate, b (W $\mathrm{m^{-2}}$) the half-saturation value of photosynthetically active radiation (PAR), and molar density of air C_{air} (mol $\mathrm{m^{-3}}$) converts units of g_s to m $\mathrm{s^{-1}}$. The eq. 10 suggests that g_s in a reference conditions (fixed D and CO_2) is constrained by plant water use and photosynthetic traits. There are readily measurable by leaf gas-exchange techniques, and widely available in literature and in plant trait databases such as TRY (Kattge et al., 2011).

For sensitivity analysis (Sect. 2.5), we determined plausible parameter ranges (Table 3) using literature, shoot gas-exchange measurements at FIHy and predictions of common leaf photosynthesis model (Farquhar et al., 1980) model coupled with eq. 9. For Scots pine, g_1 was shown to vary between 1.9 and 2.3 for different shoots measured at FIHy (Launiainen et al., 2015), while g_1 was 3.5 - 4.0 for deciduous Aspen and Birch leaves at the same site (unpublished data). These fall well within the values from global synthesis, giving mean g_1 2.35 for evergreen gymnosperm and 4.67 for deciduous angiosperm tree species (boreal biome mean g_1 2.2) (Lin et al., 2015). The A_{max} and b can be derived from shoot gas-exchange measurements, or as here by using common leaf gas-exchange model (Farquhar et al., 1980) with parameter values characteristic for boreal plants. Fig. 3 hows photosynthetic light response curves for combinations of parameter values (at reference temperature 25 $^\circ C$): maximum carboxylation velocity $V_{cmax,25}$ 40 - 70 μmol $\mathrm{m^{-2}\ s^{-1}}$; maximum electron transport rate $J_{max} = 1.9 \times V_{cmax}$ and dark respiration rate $r_d = 0.02 \times V_{cmax}$. For the specific version of Farquhar -model used, and its other 'generic' parameters see Launiainen et al. (2015).

The plausible values for A_{max} and b can be now approximated by fitting empirical light response $A_{max}\,Q_p/(Q_p+b)$ to leaf gas-exchagne model predictions. Further, as V_{cmax} and A_{max} are strongly related to leaf N (Kattge et al., 2009), using site fertility class as a proxy for A_{max} could later provide a way to infuse site type effect into spatial predictions of transpiration.

The upscaling from g_s to G_c by the proposed scheme (eq. 4 in the main paper), and the leaf gas-exchange model predictions are compared in 4. The G_c in x-axis corresponds to case $V_{cmax} = 55$ μmol $\mathrm{m^{-2}\ s^{-1}}$ and $g_1 = 2.5$ in Fig. 3 and is computed

as follows: First, a canopy with LAI = 4.0 m^2m^{-2} is divided into 100 layers and absorbed Q_p (per unit leaf area) at each layer computed assuming attenuation of Q_p exponential with attenuation coefficient $k_p = 0.6$ (T and D taken constant with height). Then, g_s for each layer is computed by the leaf gas-exchange model using local Q_p, and integrated with respect to LAI to yield G_c. The parameters for eq.4 are inferred from the leaf-scale light-response (Fig. 3) as $A_{max} = 11.6$ μmol m^{-2} and $b = 60$ Wm^{-2}. The forcing data (Q_p, D and CO_2) were taken from 1/2 h average values in July-August 2005 at FIHy site. The results show reasonably good correspondence at the sub-daily timescale. The applicability of eq. 4 at daily timescale is then indirectly explored in the main manuscript by comparison against daily dry-canopy ET measurements from ten boreal FluxNet sites.

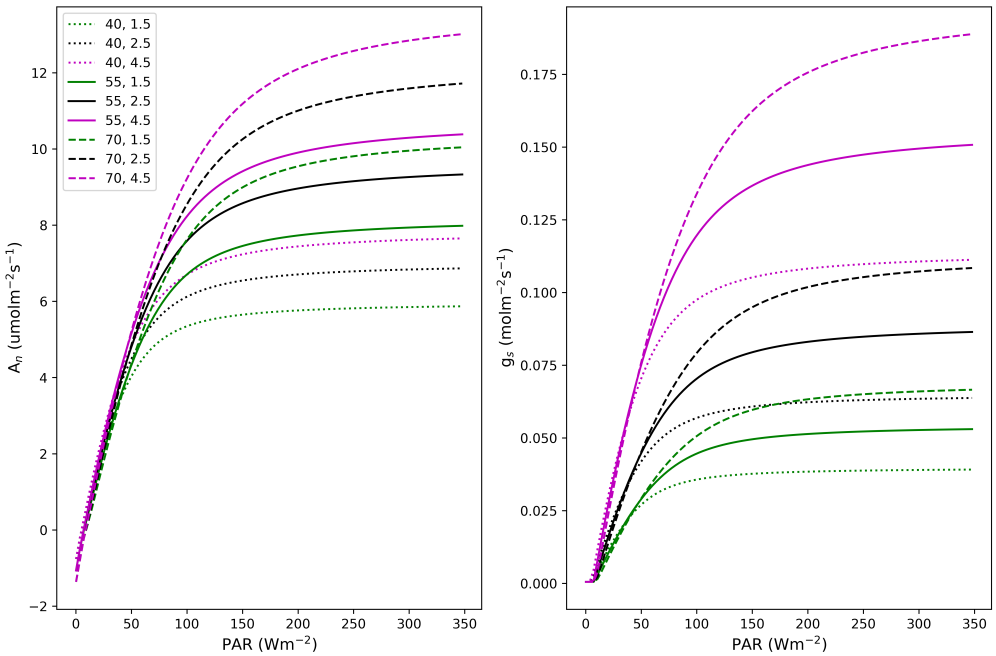

Figure 3. Photosynthetic light response and stomatal conductance predicted by a common leaf gas-exchange model for different parameter combinations. The legend gives values of V_{cmax} and g_1 for each curve. See text for details.

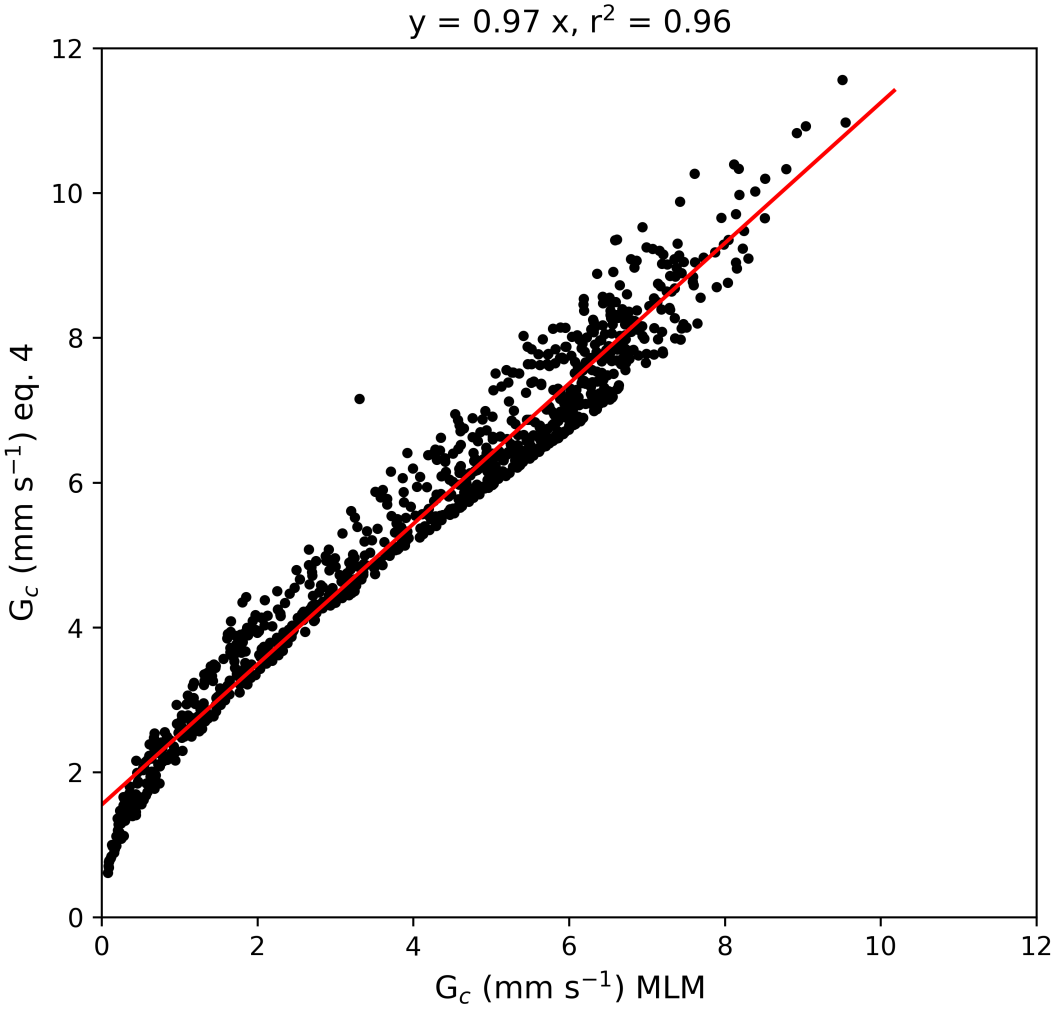

Figure 4. Canopy conductance G_c predicted by a leaf gas-exchange model combined with exponential attenuation of radiation (x-axis) and by the proposed simplification (eq. 4 in the main manuscript, y-axis). The canopy LAI = 4.0 $m^2 m^{-2}$ and the parameters of gas-exchange model correspond to case $V_{cmax} = 55$ μmol m^{-2} s^{-1} and $g_1 = 2.5$ in Fig. 3, while those in eq. 4 uses A_{max} and b inferred by fitting the light response $A_{max}\, Q_p/(Q_p + b)$ to that particular case in Fig. 3. The points show 1/2 h predictions and the red line is linear-least squares regression.

4 Snow model

Snowpack at the forest floor is described through snow water equivalent (SWE), which consists on solid (SWE_i) and liquid phases (SWE_l) (mm). Their respective mass balances are computed as

$$\frac{\Delta SWE_i}{\Delta t} = f_s\left(T_f + U_s\right) + F - M$$
$$\frac{\Delta SWE_i}{\Delta t} = \left(1 - f_s\right)\left(T_f + U_s\right) - F + M, \tag{11a}$$

where f_s is temperature-dependent fraction of precipitation falling as snow, T_f and U_s throughfall and snow unloading rates, respectively. The snowmelt M and liquid water re-freezing F (mm d^{-1}) are estimated based on degree-day approach

$$M = \min\left(SWE_i, K_m\, T_a\right), T_a < 0.0°C$$
$$F = \min\left(SWE_l, K_f\, T_a\right), T_a > 0.0°C, \tag{12a}$$

where K_m (mm d^{-1} $°C^{-1}$) is melting coefficient and freezing coefficient $K_f \sim 0.3$mm d^{-1} $°C^{-1}$ is assumed independent of stand characteristics. The snowpack can retain only a certain fraction of liquid water, and thus SWE_l is constrained to $\leq r\, SWE_i$, where $r \sim 0.05$. The excess liquid water from the snowpack is routed to soil sub-model (*Bucket*) as potential infiltration $I_{f,p}$. In snowfree conditions $I_{f,p} = T_f$.

Code and data availability. The SpaFHy source code (Python 2.7/3.6), a brief user manual and a sample dataset to run the model for a single forest stand and for a single catchment are available under MIT license at license at www.github.com/lukeecomod/spafhy_v1. Data from a Hyytiälä (FIHy) used in stand-scale evaluation is available at https://avaa.tdata.fi/web/avaa/-/smartsmear. Eddy-covariance data from other sites, and the specific discharge data used in Topmodel calibration and catchment scale evaluation can be obtained from the corresponding author. All GIS-data used in this work is openly available for whole Finland; the entry-point for obtaining GIS-data in Finland is https://www.paikkatietoikkuna.fi/?lang=en. The mNFI -data at 16 m resolution is available at http://kartta.luke.fi/index-en.html.

References

Best, M., Pryor, M., Clark, D., Rooney, G., Essery, R., Ménard, C., Edwards, J., Hendry, M., Porson, A., Gedney, N., et al.: The Joint UK Land Environment Simulator (JULES), model description–Part 1: energy and water fluxes, Geoscientific Model Development, 4, 677–699, 2011.

Bittelli, M., Campbell, G. S., and Tomei, F.: Soil Physics with Python: Transport in the Soil-Plant-Atmosphere System, OUP Oxford, 2015.

Campbell, G. S. and Norman, J. M.: Introduction to Environmental Biophysics, Springer, 2nd edn., 1998.

Choudhury, B. J. and Monteith, J.: A four-layer model for the heat budget of homogeneous land surfaces, Quarterly Journal of the Royal Meteorological Society, 114, 373–398, 1988.

Essery, R., Pomeroy, J., Parviainen, J., and Storck, P.: Sublimation of snow from coniferous forests in a climate model, Journal of Climate, 16, 1855–1864, 2003.

Farquhar, G. v., von Caemmerer, S. v., and Berry, J.: A biochemical model of photosynthetic CO2 assimilation in leaves of C3 species, Planta, 149, 78–90, 1980.

Kattge, J., Knorr, W., Raddatz, T., and Wirth, C.: Quantifying photosynthetic capacity and its relationship to leaf nitrogen content for global-scale terrestrial biosphere models, Global Change Biology, 15, 976–991, 2009.

Kattge, J., Diaz, S., Lavorel, S., Prentice, I. C., Leadley, P., Bönisch, G., Garnier, E., Westoby, M., Reich, P. B., Wright, I. J., et al.: TRY–a global database of plant traits, Global Change biology, 17, 2905–2935, 2011.

Launiainen, S., Katul, G. G., Lauren, A., and Kolari, P.: Coupling boreal forest CO2, H2O and energy flows by a vertically structured forest canopy – Soil model with separate bryophyte layer, Ecological Modelling, 312, 385–405, 2015.

Lin, Y.-S., Medlyn, B. E., Duursma, R. A., Prentice, I. C., Wang, H., Baig, S., Eamus, D., de Dios, V. R., Mitchell, P., Ellsworth, D. S., et al.: Optimal stomatal behaviour around the world, Nature Climate Change, 5, 459, 2015.

Magnani, F., Leonardi, S., Tognetti, R., Grace, J., and Borghetti, M.: Modelling the surface conductance of a broad-leaf canopy: effects of partial decoupling from the atmosphere, Plant, Cell & Environment, 21, 867–879, 1998.

Medlyn, B. E., Duursma, R. A., Eamus, D., et al.: Reconciling the optimal and empirical approaches to modelling stomatal conductance, Global Change Biology, 18, 3476–3476, 2012.

Pomeroy, J., Parviainen, J., Hedstrom, N., and Gray, D.: Coupled modelling of forest snow interception and sublimation, Hydrological Processes, 12, 2317–2337, 1998.

Saugier, B. and Katerji, N.: Some plant factors controlling evapotranspiration, Agricultural and Forest Meteorology, 54, 263–277, 1991.